Title

Fusion constructs enhance heterologous β-phellandrene production in Synechocystis sp. PCC 6803

Journal

Journal of Applied Phycology, 32(5)

ISSN

0921-8971

Authors

Valsami, Eleftheria-Angeliki
Psychogyiou, Maria Eleni
Pateraki, Angeliki
et al.

Publication Date

2020-10-01

DOI

10.1007/s10811-020-02186-1

Peer reviewed

Journal of Applied Phycology
https://doi.org/10.1007/s10811-020-02186-1

Fusion constructs enhance heterologous β-phellandrene production in *Synechocystis* sp. PCC 6803

Eleftheria-Angeliki Valsami[1] · Maria Eleni Psychogyiou[1] · Angeliki Pateraki[1] · Eleni Chrysoulaki[1] · Anastasios Melis[2] · Demetrios F. Ghanotakis[1]

Received: 2 April 2020 / Revised and accepted: 15 June 2020

Abstract

The impact of fusion genes on the overexpression of enzymes for the heterologous production of β-phellandrene by *Synechocystis* mutants was investigated. The concept of overexpression of fusion genes was used in order to overcome the low expression level of these enzymes. Various constructs of the codon-optimized gene of β-phellandrene synthase (*PHLS*), along with the gene of geranyl diphosphate synthase (*GPPS*), were incorporated into the genomic DNA of *Synechocystis* sp. PCC 6803 following fusion with the highly expressed endogenous *cpcB* and *cpcA* genes, encoding the phycocyanin β- and α-subunits, respectively. Findings in this study indicated that the utilization of a strong promoter (*cpc*) in combination with the *cpcB* as a leader sequence was not by itself sufficient for cpcB.PHLS protein overexpression in the absence of the rest of the *cpc* operon genes (*cpcA*, *cpcC2*, *cpcC1*, *cpcD*). Significantly higher expression of the CpcB.PHLS fusion protein was achieved only when all *cpc* operon genes were present. In this case, the β-phellandrene yield was substantially greater compared with strains that also expressed the *cpcB.PHLS* fusion gene in the absence of the remainder *cpc* operon genes. Interestingly, when the *cpcA* was used in the leader sequence position, the CpcA.PHLS fusion protein caused the heterologous production of a mixture of terpenoid isomers, instead of β-phellandrene. This study extends previous findings in the field and provides new insights into the use of the fusion construct technology as a heterologous protein overexpression strategy for enzymes with slow catalytic activity.

Keywords Cyanobacteria · Terpenoids · β-Phellandrene · Metabolic engineering · *Synechocystis* · Photosynthesis · Fusion proteins

Introduction

Cyanobacteria are well adapted photosynthetic microorganisms that can be found in a vast array of ecological habitats, including extreme environments (Mavroudakis et al. 2019). Due to their versatile metabolic systems and forward and reverse genetics approaches, they have been used as scaffold microorganisms with a wide range of biotechnological applications, from bioremediation and wastewater treatment to the sustainable production of a plethora of natural products (Dubey et al. 2011). A few examples include the production of bio-hydrogen (Touloupakis et al. 2016), sugars, fatty acids, pigments (chlorophyll *a*, carotenoids, phycocyanin), vitamins, and enzymes (Lau et al. 2015). Synthetic biology and metabolic engineering have made cyanobacteria ideal microbial cell factories in which photosynthesis and the associated metabolism are driven to the synthesis of bio-based chemicals and fuels (Melis 2012). The production of these molecules relies on sustainable and abundant raw materials, such as sunlight, carbon dioxide (CO_2), and water.

Unlike higher plants, cyanobacteria exhibit faster growth rates and higher photosynthetic efficiencies (Dismukes et al. 2008), are amenable to easy genetic modifications, can be grown on an industrial scale in affordable media, display easier product harvesting processes, and alleviate the competition for arable land (Ducat et al. 2011; Bentley et al. 2014; Hendry et al. 2019; Lin and Pakrasi 2019; Liu and Nielsen 2019). In addition, the genome sequences of more than 270 cyanobacterial strains are available today, making the application of -omics techniques (e.g., transcriptomics and proteomics) easier to apply (Santos-Merino et al. 2019). On the other hand, extraction and purification of natural products from

✉ Demetrios F. Ghanotakis
ghanotakis@uoc.gr

[1] Department of Chemistry, University of Crete, Voutes Campus, 70013 Heraklion, Greece

[2] Department of Plant and Microbial Biology, University of California, 111 Koshland Hall, MC-3102, Berkeley, CA 94720, USA

Published online: 06 July 2020

plant tissues have a number of limitations including the slower rates of plant growth, fluctuations in product yield depending on seasonal, weather and geographical factors, and the increasing demand for these products and the competition for land. In addition, plants contain complex mixtures of compounds with similar chemical structures. This property increases both the difficulty and cost of the extraction and purification of the desirable target compound (Kiyota et al. 2014; Kallscheuer et al. 2019). The use of cyanobacteria for the production of high-value phytochemicals has many advantages over heterotrophic microorganisms, as cyanobacteria utilize CO_2 and do not rely on other carbon sources such as sugars. Cyanobacteria offer a "green" approach since they are able to convert CO_2, a greenhouse gas, into the desired product, while the remaining cell biomass can be used as animal feed or fertilizer (Lau et al. 2015). Since cyanobacteria are the progenitors of higher plant chloroplasts and utilize the same metabolic pathways, they are an excellent choice for the expression of functionally active higher plant enzymes compared with heterotrophic microorganisms (Pattanaik and Lindberg 2015). The model organisms *Synechocystis* sp. PCC 6803 and *Synechococcus elongatus sp. PCC* 7492, *Synechococcus* sp. PCC 7002 and *Anabaena* sp. PCC 7120 are the cyanobacterial strains that have been used in several applications targeting the production of valuable compounds through metabolic engineering (Savakis and Hellingwerf 2015). During the past decades, many valuable compounds have been produced by engineered cyanobacteria. These are specialty and commodity chemicals, which can be used as biofuels or pharmaceuticals, such as ethanol (Deng and Coleman 1999; Hellingwerf and Teixeira de Mattos 2009; Gao et al. 2012), ethylene (Takahama et al. 2003; Xiong et al. 2015), acetone (Zhou et al. 2012), isopropanol (Kusakabe et al. 2013), 1,2-propanediol (Li and Liao 2013), isobutanol (Miao et al. 2017), sucrose (Ducat et al. 2012), lactic acid (Angermayr et al. 2012), fatty acids (Liu et al. 2011), and terpenoids (e.g., Betterle and Melis 2019).

Among these products, attention in our labs has been directed towards terpenoids. Terpenoids or isoprenoids are the most diverse group of natural products as they form the largest class of plant secondary metabolites. Terpenoids are essential for plant growth and metabolism and a great number of these are important secondary metabolites. They are key components of plant essential oils, steroids, phytol, and carotenoids (Chaves et al. 2016). Due to their diverse structures, biological activities, and physical and chemical properties, terpenoids are of great commercial value with many industrial applications, ranging from flavor, fragrance, and pharmaceuticals to pesticides and potentially biofuels (Chaves and Melis 2018b). In plant plastids, cyanobacteria, and microalgae, terpenoids are synthesized via the methyl-erythritol-4-phosphate (MEP) pathway, which is of prokaryotic origin (Bentley et al. 2014; Chaves and Melis 2018b). The universal precursors for terpenoid synthesis are the 5-carbon isopentenyl diphosphate (IPP) and dimethylallyl diphosphate (DMAPP) molecules (Englund et al. 2018). The head-to-tail covalent linkage of DMAPP and IPP, catalyzed by the enzyme geranyl diphosphate synthase (GPPS), results in the synthesis of the 10-carbon geranyl diphosphate (GPP), the precursor molecule for the biosynthesis of all monoterpenoids and other more complex terpenes (Englund et al. 2015). Although cyanobacteria produce a large number of longer terpenoids through the MEP pathway, they do not possess the genetic information to generate 5C hemiterpenes, 10C monoterpenes, and 15C sesquiterpenes (Van Wagoner et al. 2007). However, various 5C, 10C, and 15C terpenoids have been generated through the heterologous expression of the corresponding plant-derived terpene synthase genes (Englund et al. 2015). A few examples are isoprene (Lindberg et al. 2010; Chaves and Melis 2018a), linalool (Aprotosoaie et al. 2014), myrcene (Johnson et al. 2016), β-phellandrene (Bentley et al. 2013; Formighieri and Melis 2014b), limonene, bisabolene (Davies et al. 2014), amorphadiene (Choi et al. 2016), β-caryophyllene (Reinsvold et al. 2011), farnesene (Halfmann et al. 2014), manoyl oxide (Englund et al. 2015) and squalene (Englund et al. 2014).

More specifically, the monoterpene β-phellandrene ($C_{10}H_{16}$) is a component of many plant essential oils, including lavender, pine, grand fir, eucalyptus, and parsley. This substance has a significant commercial potential and finds applications in pharmaceuticals, flavor, fragrance, cosmetics, personal-care products, and household and industrial supplies. It also has the potential to be used as an advanced biofuel, since monoterpenes can be viewed as bio-gasoline (Melis 2017). Despite its high demand in trade and industry, β-phellandrene is quite expensive and difficult to acquire commercially, especially in high purity, without other monoterpene impurities. Heterologous production of β-phellandrene by the cyanobacterium *Synechocystis*, via the heterologous expression of the codon-optimized *Lavandula angustifolia* (lavender) β-phellandrene synthase (*PHLS*) gene, has been reported (Bentley et al. 2013). An advantage of β-phellandrene production by engineered *Synechocystis* is the spontaneous separation of this compound from the cells and the liquid medium of the culture. As a hydrophobic molecule, β-phellandrene diffused through the cells and accumulates on the surface of the liquid culture, facilitating the harvesting procedure and leading to a product free of impurities (Bentley and Melis 2012; Formighieri and Melis 2015).

However, there are barriers that need to be addressed in order to achieve the production yields required for commercial applications. Terpene synthases are secondary metabolism enzymes. One such barrier is the low product yield attributed to the slow catalytic activities of phellandrene synthase and geranyl diphosphate synthase enzymes which have a $k_{cat} = 3\ s^{-1}$ (Demissie et al. 2011; Zurbriggen et al. 2012). Another

barrier to the heterologous production of phellandrene in *Synechocystis* is the low pool level of intermediates and the competition with the endogenous terpenoid biosynthetic pathway for the GPP substrate. Geranyl diphosphate synthase does not provide enough substrate for both the endogenous metabolic pathway of terpenoids and the heterologous β-phellandrene synthase enzyme. This particular characteristic, in addition to the slow catalytic activity of the phellandrene synthase enzyme, has resulted in low product yields.

Previous studies have shown that overexpression of the transgenic proteins helps to alleviate their slow catalytic activity and result in a higher product yield (Formighieri and Melis 2015; Betterle and Melis 2019). This was achieved by the expression of phellandrene and geranyl diphosphate synthases as fusion proteins with highly expressed sequences in *Synechocystis*. The homologous *cpcB* gene, encoding the phycocyanin β-subunit and the heterologous *nptI* gene which confers resistance to kanamycin, were used as leader sequences in fusion constructs, respectively, resulting in significantly greater transgene protein accumulation and product yield (Betterle and Melis 2018, 2019).

In the present study, the fusion constructs as protein overexpression concept were further investigated and applied. More specifically, the contribution of the different *cpc* operon genes in the expression levels of the CpcB.PHLS fusion protein and the yield of β-phellandrene were studied. Additionally, the CpcA.PHLS fusion protein overexpression in *Synechocystis* was investigated. Finally, the *GPPS* gene was co-expressed as either a *cpcA.GPPS* or *cpcB.GPPS* fusion construct, along with the *cpcB.PHLS* or *cpcA.PHLS* fusion sequences, respectively, all under the control of the strong *cpc* promoter.

Materials and methods

Recombinant constructs, *Synechocystis* transformant strains

The unicellular cyanobacterium *Synechocystis* sp. PCC 6803 (*Synechocystis*), referred to as the wild type (WT), was employed as an experimental strain in the present study. The codon-optimized gene of β-phellandrene synthase (*PHLS*) from *Lavandula angustifolia* (Demissie et al. 2011; Formighieri and Melis 2014a) was used for heterologous expression in *Synechocystis* and production of β-phellandrene (β-PHL). A number of fusion constructs of the *PHLS* gene along with the gene of geranyl diphosphate synthase (*GPPS*), as well as the highly expressed endogenous *cpcB* and *cpcA* genes, in addition to a chloramphenicol resistance cassette, were generated. These constructs were incorporated into the genomic DNA of *Synechocystis* via double homologous recombination between the 500 base pairs of the upstream and downstream sequences of the *cpc* operon and expressed under the control of the native *cpc* operon promoter (Formighieri and Melis 2015). Successful synthesis of all constructs was confirmed by nucleotide sequencing. The *Δcpc Synechocystis* strain was used as the recipient strain, and transformations were performed as described by Kirst et al. (2014). Transgenic DNA copy homoplasmy and maintenance of the transformants was achieved by adding antibiotic selectable markers (30 μg mL^{-1} chloramphenicol (cmR) and/or 25 μg mL^{-1} kanamycin) into the medium of the agar plates. All experiments were repeated at least three times.

Growth conditions

All strains employed in this study were maintained on 1% w/v agar BG-11 media supplemented with 10 mM HEPES-NaOH buffer (pH 8.2) and 0.3% w/v sodium thiosulfate. Liquid cultures were grown in 25 mM phosphate-buffered BG-11 medium (pH 7.5) in a temperature-controlled chamber (28 °C), under constant aeration and light intensity of 50 μmol photons m^{-2} s^{-1}.

Genomic DNA PCR analysis

Genomic DNA templates were prepared by using Chelex 100 Resin (Biorad) as previously described (Formighieri and Melis 2014b). *Synechocystis* cells contain multiple identical circular DNA copies. Thus, complete segregation of the transgenes into all copies of *Synechocystis* genome was examined by genomic DNA PCR analysis. The oligonucleotide primer sequences used are listed in Table 1 and the genomic DNA primer hybridizing sites are presented in Fig. 1. Genomic DNA PCR analysis was performed using 5 μL of genomic DNA as a template in 25 μL PCR mix and Phusion High-Fidelity DNA Polymerase (New England Biolabs). Three independent lines of each strain were selected for further analysis.

Protein analysis

Cells from liquid cultures in the late-exponential growth phase were harvested by centrifugation at 4000×*g* for 10 min and resuspended in 5 mL of 50 mM Tris-HCl (pH 8). Cell suspensions were treated with protease inhibitor (1 mM PMSF) and disrupted by passing twice through a French press at 1500 psi. Cell lysates were centrifuged at 2250×*g* for 3 min to pellet cell debris and unbroken cells. Samples were incubated for 2 h at room temperature with an equal volume of solubilization buffer (250 mM Tris-HCl, pH 6.8, 7% w/v SDS, 20% w/v glycerol and 2 M urea). Then, samples were supplemented with β-mercaptoethanol to a final concentration of 5% and examined by SDS-PAGE and Western blot analysis. For protein visualization on SDS-PAGE, gels were stained with Coomassie

Table 1 Oligonucleotide primer sequences used in the genomic DNA PCR analysis of *Synechocystis* wild type and transformants

Primer	Oligonucleotide sequence (5 to 3)	Tm (°C)
cpc_us	GAG ATC AGT AAC AAT AAC TCT AGG GTC	56
cpc_ds	GAG ATT AGT CAT TGT TAT GGT TAG TTA ATG C	56
cpcA_Rv	GGT GGA AAC GGC TTC AGT TAA AG	58
Kan_ins_Rv	AAG GGA CAA TTG CAA ACG GG	56

Primers cpc_us, cpc_ds, and cpcA_Rv are taken from the literature (Formighieri et al. 2015; Chaves et al. 2016)

brilliant blue dye. For Western blot analysis, proteins were transferred to a nitrocellulose membrane for immunodetection and probed with PHLS- and GPPS-specific polyclonal antibodies (Formighieri and Melis 2016).

Determination of biomass accumulation

Cell growth was determined spectrophotometrically by measuring the optical density of the culture at 730 nm (OD_{730}). Biomass accumulation was determined gravimetrically by measuring the dry cell weight (DCW) of the cells.

Qualitative and quantitative determination of photosynthetic pigments

Photosynthetic pigment content was determined spectrophotometrically from the cell lysates using a Shimadzu UV-2700 UV–Vis spectrophotometer. The quantification of chlorophyll *a* and carotenoids was performed according to the protocol of Lichtenthaler (1987). Briefly, 1 mL of culture was centrifuged at 1000×*g* for 1 min. After supernatant disposal, the pellet was resuspended in 1 mL of methanol. After incubation in the dark for 15 min, the absorbance at specific wavelengths (470, 650, 665, and

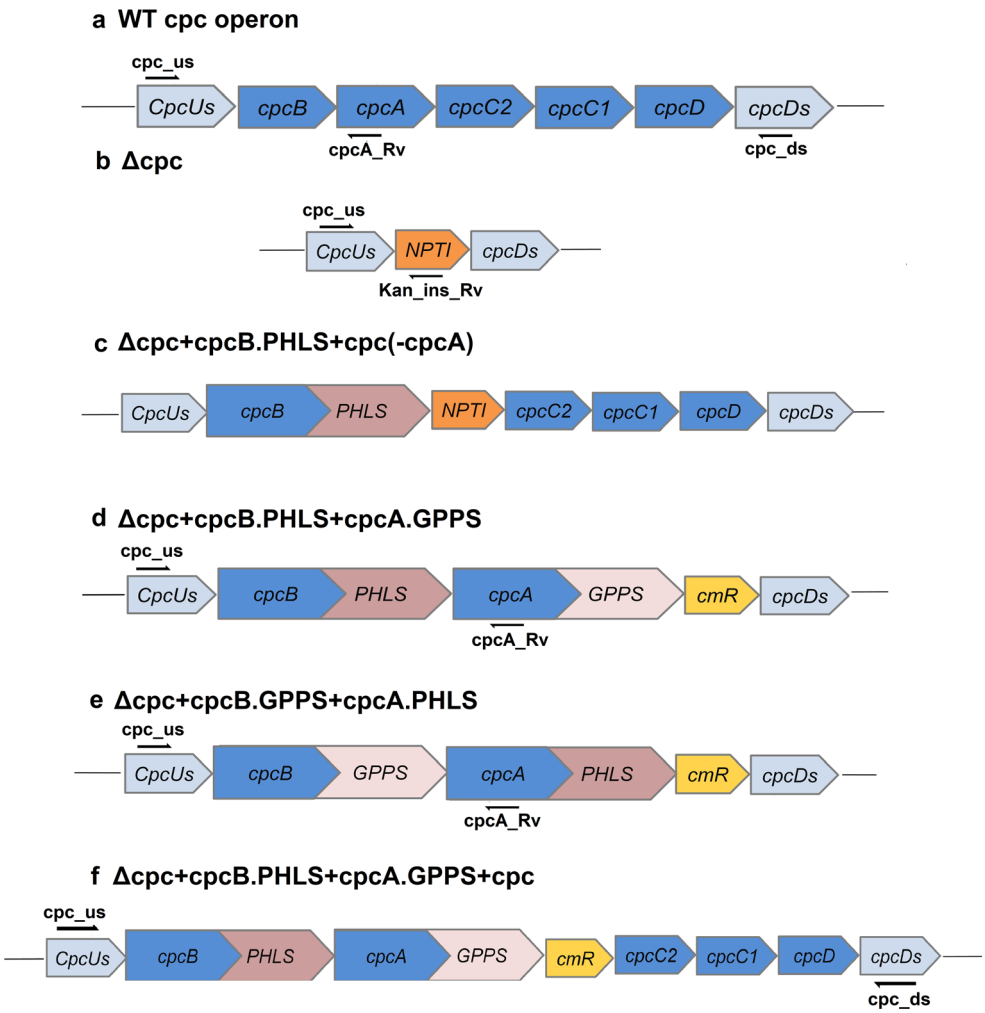

Fig. 1 Schematic illustration of the recombinant constructs used in the present work in order to replace the native *cpc* operon genes in *Synechocystis* and location of *cpc_us*, *cpcA_Rv*, *kan_ins_Rv*, and *cpc_ds* primers. **a** The *cpc* operon in *Synechocystis* wild type. **b** *Δcpc* strain used as a recipient strain in this study. **c** *Δcpc + cpcB.PHLS + cpc(−cpcA)* transformant containing the *cpcB.PHLS* fusion gene as well as the genes encoding the phycocyanin linker polypeptides (*cpcC2*, *cpcC1*, and *cpcD*), while the *cpcA* gene is absent. **d** *Δcpc + cpcB.PHLS + cpcA.GPPS* and **e** *Δcpc + cpcB.GPPS + cpcA.PHLS* have the *cpcB.PHLS*, *cpcA.GPPS*, and *cpcB.GPPS*, *cpcA.PHLS* fusion genes while the genes encoding the linker polypeptides are absent. **f** In the *Δcpc + cpcB.PHLS + cpcA.GPPS + cpc* construct, the *cpc* operon is replaced by the *cpcB.PHLS* and *cpcA.GPPS* fusion constructs in the presence of the genes encoding the phycocyanin linker polypeptides

710 nm) was determined using a Shimadzu UV-2700 UV–Vis spectrophotometer.

Photosynthetic activity measurements

Maximal photosynthetic activity (Pmax) was measured at 25 °C by using a Clark type electrode system (YSI model 5300 Biological Oxygen Monitor). Samples were illuminated with 500 μmol photons·m^{-2}·s^{-1} and the infrared part of the applied irradiation was filtered off by using a 2% $CuSO_4$ solution contained in a cuvette (4 cm path length) and placed between the actinic light source and the sample. Measurements took place under saturating carbon dioxide conditions, achieved by dissolving 0.034% w/v $NaHCO_3$ and 0.896% w/v Tricine (pH 7.6) in the cell-containing medium (Delieu and Walker 1981). The rate of oxygen evolution was recorded continuously for a period of 1 min. Maximal photosynthetic activity was expressed in mmol O_2 (mol Chl)$^{-1}$·s^{-1}.

β-Phellandrene production

Extraction and quantification of β-phellandrene from *Synechocystis* cultures were performed using established protocols (Bentley et al. 2013; Formighieri and Melis 2014b). Cells were initially centrifuged at 4500×*g* for 10 min and resuspended in 600 mL of fresh phosphate-buffered BG-11 media at an $OD_{730} = 0.5$, in a 1 L gaseous/aqueous two-phase reactor (Bentley and Melis 2012). The bioreactors were then slowly bubbled with 200 mL of 100% CO_2 gas through the bottom of the liquid culture, sealed and incubated for 48 h at 28 °C and under 50 μmol photons m^{-2} s^{-1}. β-Phellandrene was collected from the surface of the culture as previously described by Bentley et al. (2013). Briefly, 10 mL of hexane was added on top of the aqueous phase. After 2 h of incubation with gentle-stirring of the culture, the organic phase was collected. One microliter of the collected hexane layer was subjected to gas chromatography-mass spectrometry (GC-MS) analysis. Further analysis was performed by UV spectrophotometry. β-Phellandrene exhibits a characteristic absorbance spectrum with a band peaking at 232.4 nm when dissolved in hexane, while other monoterpenoids (including α-phellandrene) exhibit a specific absorbance peak at 260 nm (Bentley et al. 2013; Formighieri and Melis 2014b).

GC-MS analysis

GC-MS analysis was conducted with an Agilent 6890 gas chromatograph equipped with a cool on-column injector, an Agilent 7683 automatic liquid sampler and an Agilent 5973 inert mass selective detector. The chromatographic separation was achieved on a DB-5MS column (30 m × 0.25 mm × 0.25 μm, Agilent Technologies). Helium was used as a carrier gas at a flow rate of 1.2 mL min^{-1}. Oven temperature was initially maintained at 50 °C for 4 min, then increased to 150 °C at a rate of 4 °C min^{-1}, and finally increased to 260 °C at a rate of 20 °C min^{-1} and held at 260 °C for 5 min. The mass spectrometer was operated in electron impact mode utilizing a 70-eV ionization energy and the mass range scanned was 45–500 amu. The identification of the β-phellandrene produced by the *Synechocystis* cultures was based on a comparison of its MS data and retention time with those of a commercially available standard. Quantitation of the produced β-phellandrene was carried out by using γ-terpinene as an internal standard.

Results and discussion

Plasmid constructs and *Synechocystis* transformants

The *cpc* operon (Fig. 1a) encodes the CpcB phycocyanin β- and CpcA α-subunits and the associated linker polypeptides (CpcC2, CpcC1, and CpcD). All these assemble to form the peripheral rods of the phycobilisome light-harvesting antenna in *Synechocystis*. It has been shown that replacement of the *cpc* operon genes with the *nptI* gene conferring kanamycin resistance (Fig. 1b) abolished the assembly of the phycocyanin peripheral rods and resulted in a truncated phycobilisome antenna (Kirst et al. 2014).

The main objective of this study was to investigate whether the presence or absence of the various *cpc* operon genes affects the expression of the *cpcB.PHLS* fusion construct, as measured by the abundance of the respective protein and the yield of β-phellandrene production. Furthermore, the aim of this study was to examine the contribution of the *cpcA* gene, as a leader sequence in the protein expression of the *cpcA.PHLS* fusion construct. Geranyl diphosphate synthase (*GPPS*) gene was also introduced in the *cpc* operon as *cpcA.GPPS* and *cpcB.GPPS* fusion constructs, concurrently with the *cpcB.PHLS* and *cpcA.PHLS* fusion sequences, respectively. Thus, various fusion constructs were constructed and used to generate the corresponding transformant strains. These constructs contained the *cpcB.PHLS* or *cpcA.PHLS* fusion genes in combination with the presence or absence of the rest of the *cpc* operon-encoded subunits. The *cpcB.PHLS* + *cpcA.GPPS*, *cpcB.GPPS* + *cpcA.PHLS*, and *cpcB.PHLS* + *cpcA.GPPS* + *cpc* sequences (Fig. 1) were integrated into the *Synechocystis* genomic DNA via double homologous recombination, thus replacing the native *cpc* operon. The Δcpc+cpcB.PHLS+cpc(−cpcA) transformant (Fig. 1c) carried the fusion *cpcB.PHLS* gene, followed by the kanamycin resistance *nptI* gene and the rest of the native *cpc* operon genes *cpcC1*, *cpcC2*, and *cpcD*, while the *cpcA* gene was absent. The Δcpc+cpcB.PHLS+cpcA.GPPS (Fig. 1d) and Δcpc+cpcB.GPPS+cpcA.PHLS (Fig. 1e) transformant strains

encoding the CpcB.PHLS, CpcA.GPPS and CpcB.GPPS, CpcA.PHLS fusion proteins, respectively, were generated upon the introduction of the corresponding fusion constructs along with the chloramphenicol resistance cassette (*CmR*) into the *cpc* operon locus, while the genes encoding the phycocyanin linker polypeptides (*cpcC1*, *cpcC2*, and *cpcD*) were removed. In the Δcpc+cpcB.PHLS+cpcA.GPPS+cpc transformant (Fig. 1f), the *cpcB.PHLS* and *cpcA.GPPS* fusion genes followed by the chloramphenicol resistance cassette and the genes encoding the associated phycocyanin linker polypeptides replaced the *cpc* operon. Thus, the abovementioned *Synechocystis* transformant strains also possessed a truncated light harvesting antenna (TLA structure), as they failed to assemble phycocyanin rods, previously described by Chaves et al. (2016) and Formighieri and Melis (2015).

Genomic DNA PCR analysis

The integration of the fusion constructs in the *Synechocystis* genome and state of transgenic DNA copy homoplasmy of the transformants were tested by PCR analysis of the *Synechocystis* genomic DNA. For this purpose, primers *cpc_us*, *cpc_ds*, *cpcA_Rv*, and *Kan_ins_Rv* were used (Table 1). Primers cpc_us, cpc_ds, and cpcA_Rv are expected to generate different size products between the various transformant lines and the wild type DNA (Fig. 1a–f), while primer Kan_ins_Rv is specific to the recipient strain (Fig. 1b). In the wild type strain, primers *cpc_us* and *cpcA_Rv* anneal upstream of the *cpc* operon promoter and within the *cpcA* gene, respectively. In the wild type, they amplified a 773 bp product (Fig. 2a, b). The same primers generated single products of 2402 and 1736 bp corresponding to the *cpcB.PHLS* and *cpcB.GPPS* inserts in the Δcpc+cpcB.PHLS+cpcA.GPPS and Δcpc+cpcB.GPPS+cpcA.PHLS transformants, respectively (Fig. 2a, b). Primers cpc_us and cpc_ds, flanking the insertion site, generated a 3570 bp product in the wild type and a 1013 bp product in the Δcpc strain (Fig. 2c). In the Δcpc+cpcB.PHLS+cpcA.GPPS+cpc transformant, PCR with primers cpc_us and cpc_ds generated a larger product of 6973 bp, offering evidence of the integration of the *cpcB.PHLS* + *cpcA.GPPS* + *cpc* construct in the *cpc* locus (Fig. 2c). Primers cpc_us and Kan_ins_Rv, anneals upstream of the cpc operon and within the *nptI* sequence, respectively. Genomic DNA PCR with these primers gave a PCR product of 533 bp in the *Δcpc* strain (Fig. 2d–f). However, no PCR product could be obtained with the same

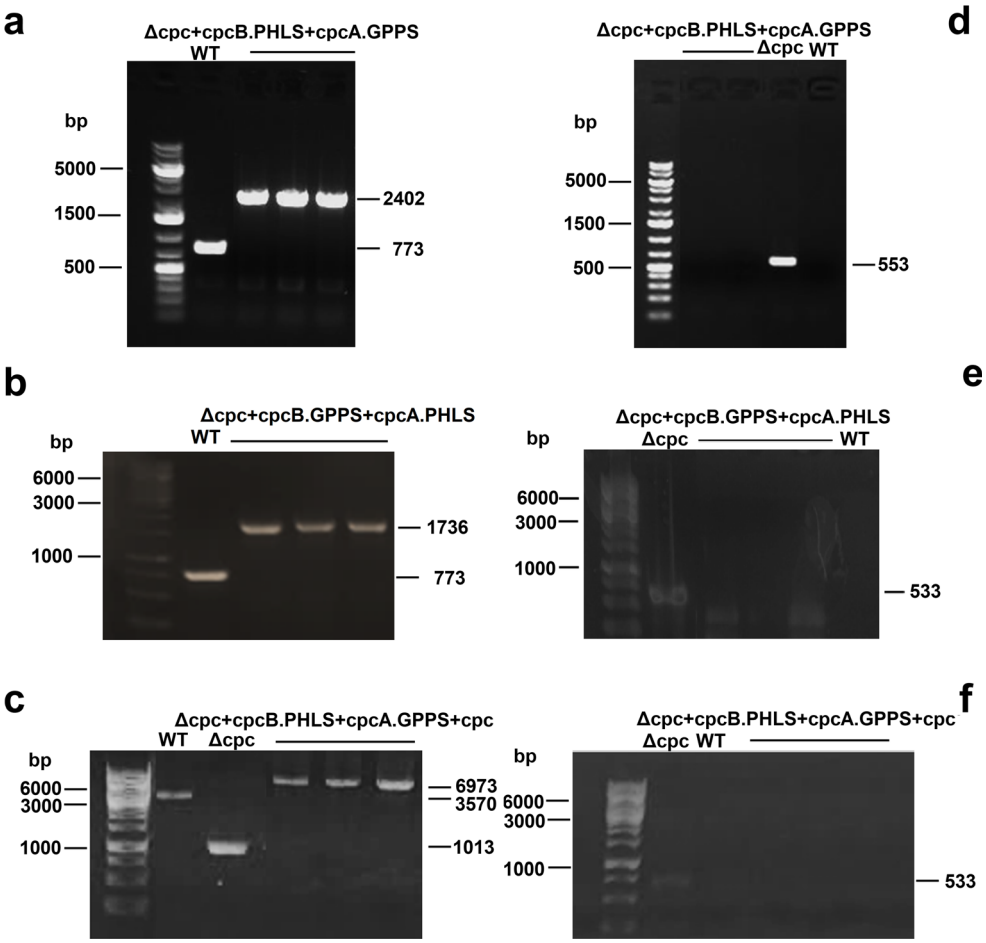

Fig. 2 Genomic DNA PCR analysis of *Synechocystis* wild type and transformant strains. **a**, **b** PCR using cpc_us and cpcA_Rv primer set and **c** PCR using cpc_us and cpc_ds primer set were used in order to examine the successful replacement of the *cpc* operon by the transgene sequences, as they generated different product sizes among the wild type, the recipient, and the different transformant strains. **d–f** PCR using cpc_us and kan_ins_Rv primer set specifically amplifies the region with the *nptI* cassette that is present only in the Δcpc strain. Thus, PCR with these primers was used to test for DNA copy homoplasmy

primers in the other transformant strains (Fig. 2d–f). The absence of a 533 bp PCR product in the *Δcpc + cpcB.PHLS + cpcA.GPPS*, *Δcpc + cpcB.GPPS + cpcA.PHLS*, and *Δcpc + cpcB.PHLS + cpcA.GPPS + cpc* transformant strains is evidence of the absence of the *nptI* gene, suggesting the attainment of transgenic DNA copy homoplasmy.

For the experiments below, a minimum of two independent lines of each transformant was isolated and tested.

Protein analysis

Protein profiles of wild type and transformant strains were examined by SDS-PAGE and Western blot analysis. In the SDS-PAGE, all strains exhibited dominant bands at 55 kD, attributed to the large subunit of Rubisco (RbcL) (Fig. 3a, b). The wild type showed two abundant proteins at 20 and 17 kD, attributed to the cpcB-encoded β-subunit of phycocyanin, and the cpcA-encoded α-subunit of phycocyanin, respectively. These two proteins are not observed in the transformants. The absence of cpcB and cpcA proteins from all the transformants confirmed that these Δcpc strains possess the TLA property (Kirst et al. 2014). The Δcpc+cpcB.PHLS+cpcA.GPPS, Δcpc+cpcB.GPPS+cpcA.PHLS, and Δcpc+cpcB.PHLS+cpcA.GPPS+cpc transformants exhibited faint bands at approximately 23 kD attributed to the expression of the chloramphenicol resistance protein. The Δcpc+cpcB.PHLS+cpc(−cpcA) and two independent lines of the Δcpc+cpcB.PHLS+cpcA.GPPS strain showed faint bands at 75 kD attributed to the CpcB.PHLS fusion protein (Fig. 3a). The same faint bands were observed in three independent lines of the Δcpc+cpcB.GPPS+cpcA.PHLS strain, attributed to the CpcA.PHLS transgenic protein. These results indicated a low transgenic protein expression in these strains. However, substantial amounts of the heterologous CpcB.PHLS

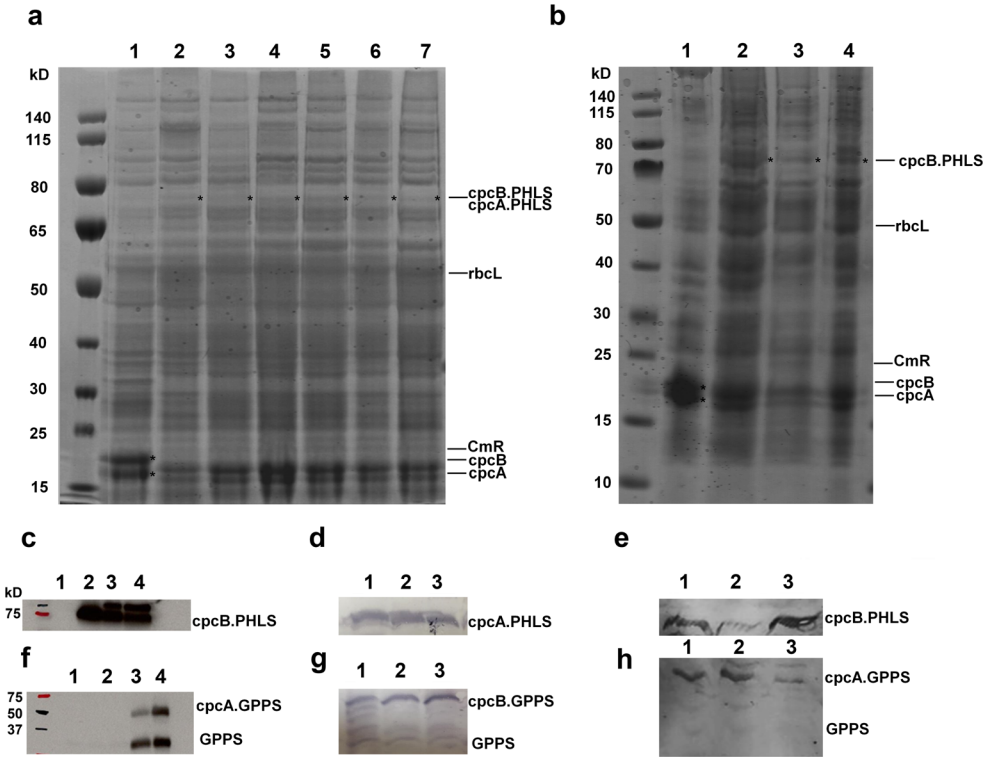

Fig. 3 Protein analysis of total protein extracts from *Synechocystis* wild type and transformant strains. **a** SDS-PAGE analysis of WT (*lane 1*), Δcpc+cpcB.PHLS+cpc(−cpcA) (*lane 2*), three independent Δcpc+cpcB.GPPS+cpcA.PHLS transformant lines (*lanes 3–5*), and two independent Δcpc+cpcB.PHLS+cpcA.GPPS transformant lines (*lanes 6–7*). **b** SDS-PAGE analysis of total protein extracts. *Lane 1*, WT; *lanes* 2–4, three independent Δcpc+cpcB.PHLS+cpcA.GPPS+cpc transformant lines. **c** Western blot analysis of protein extracts from *Synechocystis* transformant strains, probed with specific polyclonal antibodies raised against the PHLS protein. Lane 1, WT; *lane 2*, Δcpc+cpcB.PHLS+cpc(−cpcA); *lanes 3–4*, two independent Δcpc+cpcB.PHLS+cpcA.GPPS transformant lines. **d** Western blot analysis of protein extracts from three independent Δcpc+cpcB.GPPS+cpcA.PHLS transformant lines (*lanes 1–3*), probed with specific polyclonal antibodies against the PHLS protein. **e** Western blot analysis of protein extracts from three independent Δcpc+cpcB.PHLS+cpcA.GPPS+cpc transformant lines (*lanes 1–3*), probed with specific polyclonal antibodies against the PHLS protein. **f** Western blot analysis of protein extracts from *Synechocystis* transformant strains, probed with specific polyclonal antibodies against the GPPS protein. *Lane 1*, WT; lane 2, Δcpc+cpcB.PHLS+cpc(−cpcA); *lanes 3–4*, two independent Δcpc+cpcB.PHLS+cpcA.GPPS transformant lines. **g** Western blot analysis of protein extracts from three independent Δcpc+cpcB.GPPS+cpcA.PHLS transformant lines (*lanes 1–3*), probed with specific polyclonal antibodies against the GPPS protein. **h** Western blot analysis of protein extracts from three independent Δcpc+cpcB.PHLS+cpcA.GPPS+cpc transformant lines (*lanes 1–3*), probed with specific polyclonal antibodies against the GPPS protein

recombinant protein were observed in three Δcpc+cpcB.PHLS+cpcA.GPPS+cpc transformant lines (Fig. 3b). In this strain, the *cpcB.PHLS* fusion genes, the genes that encode the linker polypeptides (*cpcC2*, *cpcC1*, *cpcD*), as well as the *cpcA* gene, in the form of *cpcA.GPPS* fusion gene, were expressed. These observations suggested that the CpcB.PHLS fusion protein is expressed in significant amounts and is evident in the SDS-PAGE gel as a dominant band, not only when the *cpcA* gene is present but also when all the rest of the *cpc* operon genes as well.

Western blot analysis with specific polyclonal antibodies against the PHLS and GPPS proteins confirmed the presence of the heterologous PHLS and GPPS fusion proteins in *Synechocystis* transformant strains (Fig. 3c–h). More specifically, a strong cross reaction of the PHLS polyclonal antibodies was observed with a protein band at 75 kD in the Δcpc+cpcB.PHLS+cpc(−cpcA) and all lines of Δcpc+cpcB.PHLS+cpcA.GPPS and Δcpc+cpcB.PHLS+cpcA.GPPS+cpc transformants, attributed to the CpcB.PHLS fusion protein (Fig. 3c, e). The same results were observed in three lines of Δcpc+cpcB.GPPS+cpcA. PHLS transformant attributed to the cpcA.PHLS fusion protein (Fig. 3d). A cross-reaction of the GPPS polyclonal antibody was observed with a protein band at 53 kD in all lines of Δcpc+cpcB.PHLS+cpcA.GPPS, Δcpc+cpcB.PHLS+cpcA.GPPS+cpc, and Δcpc+cpcB.GPPS+cpcA.PHLS transformants attributed to the cpcA.GPPS and cpcB.GPPS fusion proteins, respectively (Fig. 3f–h).

Further evidence for the identity of these protein bands was obtained upon the analysis of the bands corresponding to the fusion proteins (CpcB.PHLS, CpcA.GPPS, CpcB.GPPS, and CpcA.PHLS) by using ESI MS/MS (Orbitrap Elite and Q executive). In all transformants, a number of peptides corresponding both to the leader and target sequences in the fusion proteins were identified (data not shown).

These results provided evidence for the heterologous expression of PHLS and GPPS fusion proteins in *Synechocystis* transformants generated in the present work.

Growth, biomass accumulation, and photosynthesis characteristics of *Synechocystis* transformants

The cell growth and biomass accumulation were determined spectrophotometrically by measuring the optical density of the cultures at 730 nm (Fig. 4a), and dry cell weight (Fig. 4b) after 48 h of cultivation in the 1 L gaseous/aqueous two-phase reactor under 50 μmol photons m^{-2} s^{-1} light intensity. As shown in Fig. 4a, all transformants exhibited similar and slightly slower growth rates than the wild type strain. This was attributed to the truncated light-harvesting antenna size of the Δcpc strains, which limits the rate of light absorption by the photosystems, hence the rate of cell growth (Kirst et al. 2014). Furthermore, it was previously reported that the slower growth of *Synechocystis* transformants, compared with the wild type strain, could arise because of slower rates of carbon partitioning to biomass accumulation, as a result of carbon flux deflection to β-phellandrene production by these strains (Du et al. 2017; Chaves and Melis 2018a; Betterle and Melis 2019).

The determination of the photosynthetic pigment content in the various transformants was achieved by analyzing the visible spectrum of cell lysates (Fig. 5a**)**. All transformants and the wild type strain showed the characteristic peak at 680 nm, attributed to Q band of chlorophyll α, an absorbance peak at 435 nm, attributed to the Soret absorption band of chlorophyll *a* with contributions from carotenoids and bilins, and a shoulder at 470 nm also attributed to carotenoids. The characteristic

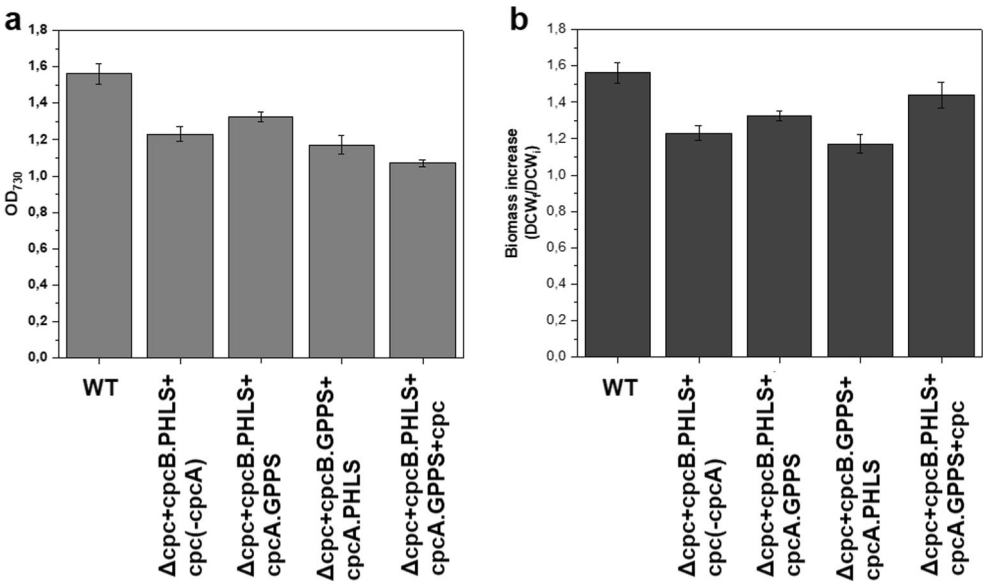

Fig. 4 Cell growth and biomass accumulation of *Synechocystis* wild type and transformant strains were measured by optical density of the culture at 730 nm (OD_{730}) and by dry cell weight (DCW) after 48 h incubation of the cultures in a gaseous/aqueous two-phase bioreactor filled with 200 mL of 100% CO_2, at 28 °C and placed under continuous illumination at 50 μmol photons m^{-2} s^{-1}

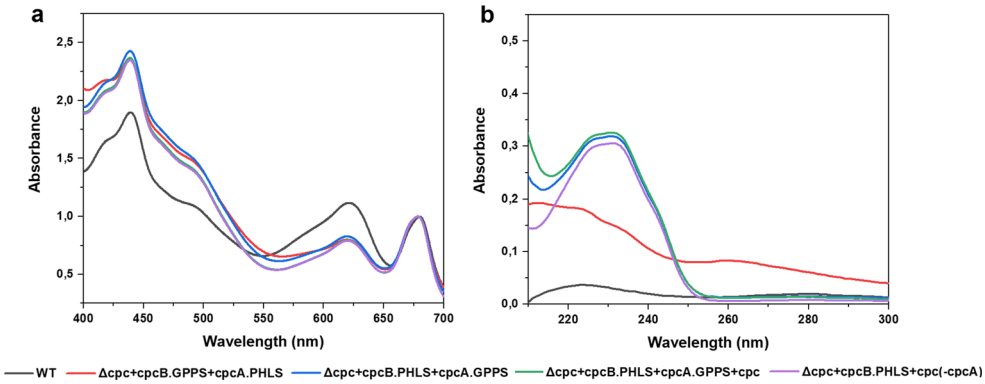

Fig. 5 **a** Normalized absorbance spectra of cell lysates were measured for the determination of the pigment content in wild type and transformant strains. **b** Absorbance spectra in the UV region of the hexane extracts from wild type and various transformant strain cultures. β-Phellandrene has a characteristic absorbance spectrum with a maximum at 232.4 nm

peak of phycocyanin at 625 nm observed in the spectrum of the wild type strain was significantly lower in all transformant strains attributed to the replacement of the *cpc* operon. This is due to the absence of the phycocyanin pigment but the presence of allophycocyanin as the only phycobilisome pigment in the modified *Synechocystis* antenna (Kirst et al. 2014). These observations, in combination with the absence of cpcB and cpcA proteins evidenced in the SDS-PAGE gel, indicate the successful deletion of the *cpc* operon and confirm the TLA phenotype in all transformant strains. These results were imprinted in the transformants' phenotype that had green coloration instead of the blue-green of the wild type strain (not shown). The carotenoid to chlorophyll *a* ratio was found to be significantly higher in the Δcpc+cpcB.PHLS+cpc(−cpcA), Δcpc+cpcB.PHLS+cpcA.GPPS and Δcpc+cpcB.GPPS+cpcA.PHLS transformants compared with that in the wild type, while the Δcpc+cpcB.PHLS+cpcA.GPPS+cpc transformant has a similar Car/Chl ratio to that of the wild type (Table 2).

Regarding the photosynthetic efficiency of mutants, the Δcpc+cpcB.PHLS+cpc(−cpcA), Δcpc+cpcB.PHLS+cpcA.GPPS, and Δcpc+cpcB.GPPS+cpcA.PHLS transformants exhibited a higher rate of photosynthetic oxygen evolution, expressed as mmol O_2 (mol Chl)$^{-1}$ s^{-1}, compared with the wild type (Table 2). This increase was found to be approximately 37% for the Δcpc+cpcB.PHLS+cpc(−cpcA) and Δcpc+cpcB.GPPS+cpcA.PHLS transformants and 35% for the Δcpc+cpcB.PHLS+cpcA.GPPS strain. In contrast, the rate of photosynthetic oxygen evolution of Δcpc+cpcB.PHLS+cpcA.GPPS+cpc strain was relatively similar to that of the wild type.

β-Phellandrene production

The spectrophotometric analysis of hexane extracts from cultures of the abovementioned strains showed the characteristic absorbance maximum of β-phellandrene at 232.4 nm (Fig. 5b).

Gas chromatograms of hexane extract from the surface of the Δcpc+cpcB.PHLS+cpc(−cpcA), Δcpc+cpcB.PHLS+cpcA.GPPS, and Δcpc+cpcB.PHLS+cpcA.GPPS+cpc cultures are shown in Fig. 6. A peak with a retention time of 12.45 min was evident in all chromatograms. This peak was confirmed to correspond to β-phellandrene, as shown in the gas chromatogram of the commercial β-phellandrene standard under the same GC operating conditions (Fig. 6a). To clarify this observation, further analysis with mass spectrometry was carried out. Figure 7 shows the comparison of the MS spectra of the chromatographic peak with retention time 12.45 min. The produced fragments (m/z = 136, 91 and 77) are consistent with those of the fragmentation patterns of the β-phellandrene standard solution (Fig. 7a), as well as previous studies in the literature (Bentley et al. 2013).

Overall, these results showed the successful heterologous production of β-phellandrene from the Δcpc+cpcB.PHLS+

Table 2 Pigment analysis and rates of photosynthetic oxygen evolution measurements of *Synechocystis* wild type and transformant strains following an incubation period of 48 h in gaseous/aqueous two-phase bioreactors filled with 200 mL of 100% CO_2, at 28 °C and under continuous illumination of 50 μmol photons m^{-2} s^{-1}

Strain	Car/Chl	Rate of photosynthetic oxygen evolution, mmol O_2 (mol Chl)$^{-1}$ s^{-1}
WT	0.40 ± 0.03	23.89 ± 1.20
Δcpc + cpcB.PHLS + cpc(−cpcA)	0.76 ± 0.07	32.90 ± 1.90
Δcpc + cpcB.PHLS + cpcA.GPPS	0.92 ± 0.05	32.16 ± 1.45
Δcpc + cpcB.GPPS + cpcA.PHLS	0.89 ± 0.09	32.77 ± 0.63
Δcpc + cpcB.PHLS + cpcA.GPPS + cpc	0.35 ± 0.01	21.03 ± 0.57

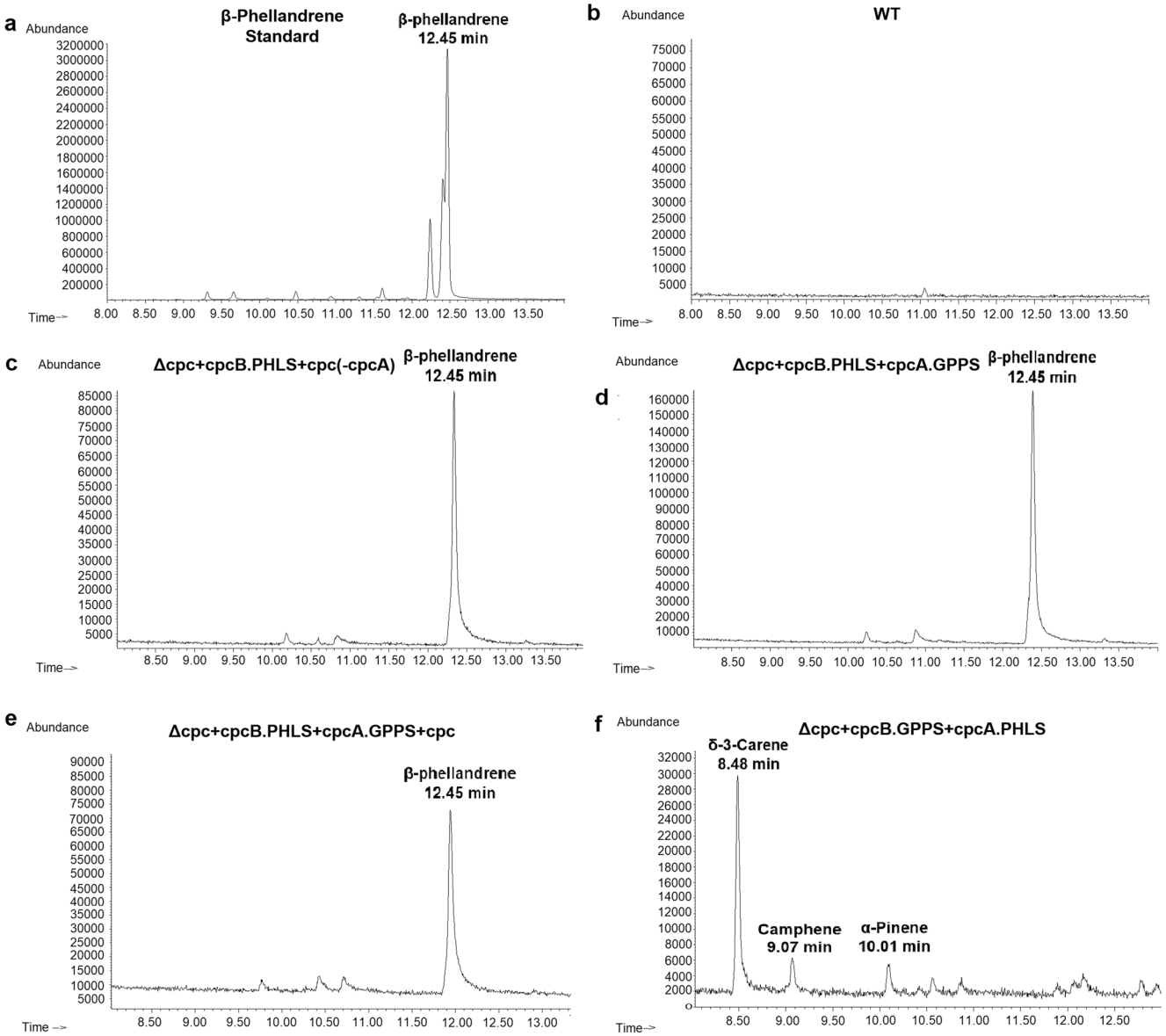

Fig. 6 Gas chromatography analysis of the hexane extracts. **a** GC analysis of a commercially available β-phellandrene standard. **b** GC analysis of *Synechocystis* wild type. **c–f** GC analysis of Δcpc+cpcB.PHLS+cpc(−cpcA), Δcpc+cpcB.PHLS+cpcA.GPPS, and Δcpc+cpcB.PHLS+cpcA.GPPS+cpc strains showing the dominant β-phellandrene peak with a retention time of 12.45 min. Also shown is the GC analysis of the hexane extracts from the Δcpc+cpcB.GPPS+cpcA.PHLS transformant culture, comprising δ-3-carene with a retention time of 8.48 min as the main monoterpene generated

cpc(−cpcA), Δcpc+cpcB.PHLS+cpcA.GPPS, and Δcpc+cpcB.PHLS+cpcA.GPPS+cpc transformants. As a negative control, wild type culture extracts were examined and found not to produce β-phellandrene, as expected (Fig. 5b, 6b).

Interestingly, the Δcpc+cpcB.GPPS+cpcA.PHLS strain was found to produce a mixture of isoprenoids. Most abundant was the accumulation of δ-3-carene, followed by camphene and α-pinene, which were detected in the gas chromatogram (Fig. 6f) instead of β-phellandrene. This observation was also accompanied by changes in the UV spectrum, where a broad spectral band (instead of the distinct β-phellandrene peak at 232.4 nm) was observed (Fig. 5b). This is a potentially important finding because this was the first time that the *PHLS* gene was fused with the *cpcA* gene. Previous studies used the *psbA2*, *cpcB*, or the *nptI* genes, as leader sequences for the expression of PHLS, leading to the specific synthesis of β-phellandrene (Bentley et al. 2013; Formighieri and Melis 2015). The discrepancy in this work can possibly be attributed to the fusion of the *PHLS* gene in the 3′-end of the *cpcA* sequence and the translation of the *cpcA.PHLS* sequence as one peptide. The tertiary configuration of the CpcA.PHLS protein may have altered the enzyme's catalytic properties, leading to the synthesis of alternative monoterpenes. These results are consistent with the notion

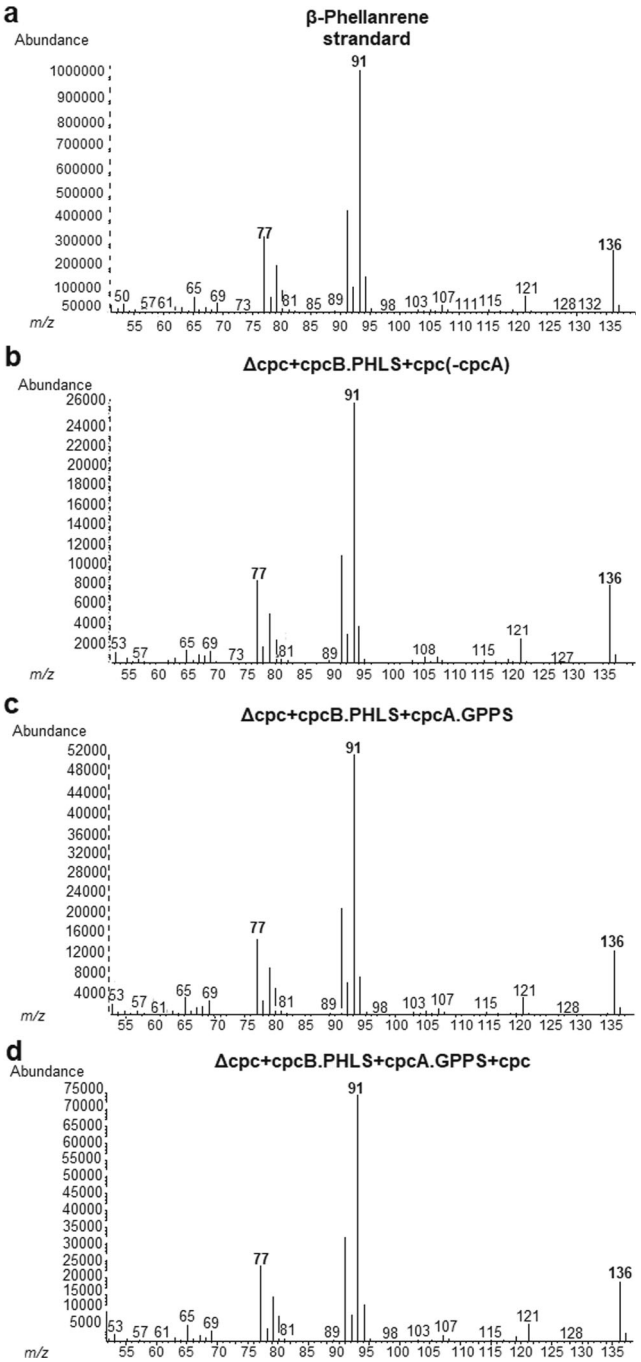

Fig. 7 Mass spectra of the chromatographic peak with retention time 12.45 min. **a** MS analysis of the GC peak with retention time 12.45 min of the commercially available β-phellandrene standard. **b–d** MS analysis of the GC peak of extracts from the Δcpc+cpcB.PHLS+cpc(−cpcA), Δcpc+cpcB.PHLS+cpcA.GPPS, and Δcpc+cpcB.PHLS+cpcA.GPPS+cpc transformant strains

that β-phellandrene synthase (PHLS) genes from different plants, when expressed in *Synechocystis*, enable synthesis of variable monoterpene hydrocarbon blends (Formighieri and Melis 2018).

In related literature, it was reported that using highly homologous or heterologous genes in *Synechocystis* (e.g., *cpcB* or *nptI* and *cmR* genes), as leader sequences in fusion constructs, leads to overexpression of the respective fusion proteins (Betterle and Melis 2018, 2019). More specifically, the highly expressed sequence, when used as a leader sequence in a fusion construct, was found to enhance the ribosome migration and translation through the entirety of the fusion sequence (Formigheiri and Melis 2016; Chaves et al. 2017). However, the results in the present study showed that the *cpcA* gene as a leader sequence does not lead to the production of β-phellandrene, but to a monoterpene hydrocarbon mixture of three β-phellandrene structural isomers. More work needs to be done in order to further investigate and explain this finding.

The β-phellandrene production yields of the different transformants are shown in Table 3. β-Phellandrene yields are expressed relative to the dry cell weight that accumulated during the incubation period of 48 h and are expressed on the basis of dry cell weight (DCW) or Chl *a* accumulation during the same period of time. The Δcpc+cpcB.PHLS+cpc(−cpcA) transformant yielded an average of 0.28 mg β-phellandrene (g DCW)$^{-1}$. Although the PHLS enzyme is expressed as a cpcB.PHLS fusion protein, under the control of the strong *cpc* promoter, the product's yield is relatively low. As mentioned in the literature, the selection of a strong promoter could result in faster rates of transcription but not into a significantly higher expression of the PHLS protein (Formighieri and Melis 2016). In contrast, the Δcpc+cpcB.PHLS+cpcA.GPPS yield of β-phellandrene was doubled to about 0.55 mg (g DCW)$^{-1}$. This could be attributed to the expression of the *GPPS* gene as a fusion gene of *cpcA.GPPS*, in the same operon with the *PHLS* gene. It is known that the GPPS enzyme in *Synechocystis* cannot provide enough geranyl diphosphate as a substrate of the PHLS enzyme, due to low expression level and activity (Formighieri and Melis 2016). It has been reported that expression of the GPPS as a fusion protein with a highly expressed sequence in *Synechocystis*, such as the

Table 3 β-Phellandrene production measurements of *Synechocystis* transformants after the incubation period of 48 h in gaseous/aqueous two-phase bioreactor filled with 200 mL of 100% CO_2, at 28 °C and under continuous illumination of 50 μmol photons m^{-2} s^{-1}. The produced β-phellandrene is expressed as mg of β-phellandrene in correlation to the dry cell weight that accumulated between the incubation period (yield) as well as μg of β-phellandrene in relation to the concentration of the chlorophyll *α* that the transformants contained after the incubation period

Strain	β-Phellandrene, yield mg (g DCW)$^{-1}$	β-Phellandrene, μg (mg Chl)$^{-1}$
Δcpc + cpcB.PHLS + cpc(−cpcA)	0.28 ± 0.00	22.60 ± 1.60
Δcpc + cpcB.PHLS + cpcA.GPPS	0.55 ± 0.03	36.19 ± 8.70
Δcpc + cpcB.PHLS + cpcA.GPPS + cpc	1.11 ± 0.01	52.59 ± 0.90

NptI protein, results in the overexpression of the GPPS fusion construct and finally enhances the β-phellandrene production (Betterle and Melis 2018, 2019). Our results suggest that CpcA as a leader sequence in a GPPS fusion configuration could also enhance the β-phellandrene yield. Furthermore, an important observation is that although both transformants (Δcpc+cpcB.PHLS+cpc(−cpcA) and Δcpc+cpcB.PHLS+cpcA.GPPS) expressed the PHLS enzyme as a CpcB.PHLS fusion protein, expression levels and product yields were not high. Interestingly, the Δcpc+cpcB.PHLS+cpcA.GPPS+cpc produced a higher average of 1.11 mg β-phellandrene per g DCW. The substantially greater β-phellandrene production in the latter could be attributed to the expression of the *cpcB.PHLS* and *cpcA.GPPS* fusion genes, as well as the expression of the rest *cpc* operon genes (*cpcC2*, *cpcC1*, and *cpcD*). A comparison of these results and the protein analysis results, where the expression of CpcB.PHLS fusion protein was higher in the last strain, revealed the significance of the presence of all the *cpc* operon genes in the expression of the *cpcB.PHLS* fusion gene, and finally in the production of β-phellandrene.

Conclusions

The present work provided a deeper insight into the *cpc* operon fusion protein overexpression concept. Various "*Δcpc*" transformants have been generated that contained the *cpcB.PHLS* or *cpcA.PHLS* fusion genes, used in combination with the presence or absence of the remaining *cpc* genes. All the transformants exhibited the TLA phenotype. All strains were found to grow efficiently and most of them produced β-phellandrene. The results of the present study showed that the construction of the *cpcB.PHLS* fusion gene and its expression under the native, strong *cpc* promoter does not necessarily result in the overexpression of the corresponding protein. The expression of the cpcB.PHLS fusion protein in substantial amounts was achieved only when all *cpc* operon genes were present. In this case, the β-phellandrene yield was substantially greater compared with strains that also expressed the *cpcB.PHLS* fusion gene, albeit in the absence of the other *cpc* operon genes. Another interesting finding is that although the use of *cpcB* gene, as a leader sequence in the fusion *cpcB.PHLS* construct, resulted in successful β-phellandrene production, the *cpcA* sequence, when used as a leader sequence, leads to a mixture of three β-phellandrene structural isomers. The work has also demonstrated that the heterologous expression of the *GPPS* gene resulted in an increased β-phellandrene production. These results extend previous findings in the field and provide new unique insights into the use of the fusion construct technology as a protein overexpression strategy for heterologous enzymes with low catalytic activity.

Acknowledgments The authors wish to thank Dr. Cinzia Formighieri for making available the cpcB.PHLS+cpcA.GPPS construct and the Δcpc+cpcB.PHLS+cpc(-cpcA) strain, Dr. M. Apostolaki for helping with the GC-MS measurements, Prof. G. Tsiotis and Prof. I. Pavlidis for valuable discussions, and Dr. J. D. Langer and I. Wuellenweber (Max-Planck-Institut for Biophysics Frankfurt am Main) for their help in protein characterization.

Funding information This research was co-financed by Greece and the European Union (European Social Fund - ESF) through the Operational Programme "Human Resources Development, Education and Lifelong Learning" in the context of the project "Scholarships programme for post-graduate studies - 2nd Study Cycle" (MIS-5003404), implemented by the State Scholarships Foundation (IKΥ).

Compliance with ethical standards

Conflict of interest The authors declare that they have no conflict of interest.

References

Angermayr SA, Paszota M, Hellingwerf KJ (2012) Engineering a cyanobacterial cell factory for production of lactic acid. Appl Environ Microbiol 78:7098–7106

Aprotosoaie AC, Hăncianu M, Costache I-I, Miron A (2014) Linalool: a review on a key odorant molecule with valuable biological properties. Flavour Frag J 29:193–219

Bentley FK, García-Cerdán JG, Chen H-C, Melis A (2013) Paradigm of monoterpene (β-phellandrene) hydrocarbons production via photosynthesis in cyanobacteria. BioEnergy Res 6:917–929

Bentley FK, Melis A (2012) Diffusion-based process for carbon dioxide uptake and isoprene emission in gaseous/aqueous two-phase photobioreactors by photosynthetic microorganisms. Biotechnol Bioeng 109:100–109

Bentley FK, Zurbriggen A, Melis A (2014) Heterologous expression of the mevalonic acid pathway in cyanobacteria enhances endogenous carbon partitioning to isoprene. Mol Plant 7:71–86

Betterle N, Melis A (2018) Heterologous leader sequences in fusion constructs enhance expression of geranyl diphosphate synthase and yield of beta-phellandrene production in cyanobacteria (*Synechocystis*). ACS Synth Biol 7:912–921

Betterle N, Melis A (2019) Photosynthetic generation of heterologous terpenoids in cyanobacteria. Biotechnol Bioeng 116:2042–2051

Chaves JE, Melis A (2018a) Biotechnology of cyanobacterial isoprene production. Appl Microbiol Biotechnol 102:6451–6458

Chaves JE, Melis A (2018b) Engineering isoprene synthesis in cyanobacteria. FEBS Lett 592:2059–2069

Chaves JE, Romero PR, Kirst H, Melis A (2016) Role of isopentenyl-diphosphate isomerase in heterologous cyanobacterial (*Synechocystis*) isoprene production. Photosynth Res 130:517–527

Chaves JE, Rueda-Romero P, Kirst H, Melis A (2017) Engineering isoprene synthase expression and activity in cyanobacteria. ACS Synth Biol 6:2281–2292

Choi SY, Lee HJ, Choi J, Kim J, Sim SJ, Um Y, Kim Y, Lee TS, Keasling JD, Woo HM (2016) Photosynthetic conversion of CO_2 to farnesyl diphosphate-derived phytochemicals (amorpha-4,11-diene and squalene) by engineered cyanobacteria. Biotechnol Biofuels 9:202

Davies FK, Work VH, Beliaev AS, Posewitz MC (2014) Engineering limonene and bisabolene production in wild type and a glycogen-deficient mutant of *Synechococcus* sp. PCC 7002. Front Bioeng Biotechnol 2:21

Delieu T, Walker DA (1981) Polarographic measurements of photosynthetic oxygen evolution by leaf disks. New Phytol 89:165–178

Demissie ZA, Sarker LS, Mahmoud SS (2011) Cloning and functional characterization of beta-phellandrene synthase from *Lavandula angustifolia*. Planta 233:685–696

Deng MD, Coleman JR (1999) Ethanol synthesis by genetic engineering in cyanobacteria. Appl Environ Microbiol 65:523–528

Dismukes GC, Carrieri D, Bennette N, Ananyev GM, Posewitz MC (2008) Aquatic phototrophs: efficient alternatives to land-based crops for biofuels. Curr Opin Biotechnol 19:235–240

Du W, Angermayr SA, Jongbloets JA, Molenaar D, Bachmann H, Hellingwerf KJ, Branco Dos Santos F (2017) Nonhierarchical flux regulation exposes the fitness burden associated with lactate production in *Synechocystis* sp. PCC6803. ACS Synth Biol 6:395–401

Dubey J, Mehra S, Tiwari P, Bishwas A (2011) Potential use of cyanobacterial species in bioremediation of industrial effluents. Afr J Biotechnol 10:1125–1132

Ducat DC, Avelar-Rivas JA, Way JC, Silver PA (2012) Rerouting carbon flux to enhance photosynthetic productivity. Appl Environ Microbiol 78:2660–2668

Ducat DC, Way JC, Silver PA (2011) Engineering cyanobacteria to generate high-value products. Trends Biotechnol 29:95–103

Englund E, Andersen-Ranberg J, Miao R, Hamberger B, Lindberg P (2015) Metabolic engineering of *Synechocystis* sp. PCC 6803 for production of the plant diterpenoid manoyl oxide. ACS Synth Biol 4:1270–1278

Englund E, Pattanaik B, Ubhayasekera SJ, Stensjo K, Bergquist J, Lindberg P (2014) Production of squalene in *Synechocystis* sp. PCC 6803. PLoS one 9:e90270

Englund E, Shabestary K, Hudson EP, Lindberg P (2018) Systematic overexpression study to find target enzymes enhancing production of terpenes in *Synechocystis* PCC 6803, using isoprene as a model compound. Metab Eng 49:164–177

Formighieri C, Melis A (2014a) Carbon partitioning to the terpenoid biosynthetic pathway enables heterologous beta-phellandrene production in *Escherichia coli* cultures. Arch Microbiol 196:853–861

Formighieri C, Melis A (2014b) Regulation of beta-phellandrene synthase gene expression, recombinant protein accumulation, and monoterpene hydrocarbons production in *Synechocystis* transformants. Planta 240:309–324

Formighieri C, Melis A (2015) A phycocyanin.phellandrene synthase fusion enhances recombinant protein expression and beta-phellandrene (monoterpene) hydrocarbons production in *Synechocystis* (cyanobacteria). Metab Eng 32:116–124

Formighieri C, Melis A (2016) Sustainable heterologous production of terpene hydrocarbons in cyanobacteria. Photosynth Res 130:123–135

Formighieri C, Melis A (2018) Cyanobacterial production of plant essential oils. Planta 248:933–946

Gao Z, Zhao H, Li Z, Tan X, Lu X (2012) Photosynthetic production of ethanol from carbon dioxide in genetically engineered cyanobacteria. Energy Environ Sci 5:9857–9865

Halfmann C, Gu L, Gibbons W, Zhou R (2014) Genetically engineering cyanobacteria to convert CO_2, water, and light into the long-chain hydrocarbon farnesene. Appl Microbiol Biotechnol 98:9869–9877

Hellingwerf KJ, Teixeira de Mattos MJ (2009) Alternative routes to biofuels: light-driven biofuel formation from CO_2 and water based on the 'photanol' approach. J Biotechnol 142:87–90

Hendry JI, Bandyopadhyay A, Srinivasan S, Pakrasi HB, Maranas CD (2019) Metabolic model guided strain design of cyanobacteria. Curr Opin Biotechnol 64:17–23

Johnson TJ, Gibbons JL, Gu L, Zhou R, Gibbons WR (2016) Molecular genetic improvements of cyanobacteria to enhance the industrial potential of the microbe: a review. Biotechnol Prog 32:1357–1371

Kallscheuer N, Classen T, Drepper T, Marienhagen J (2019) Production of plant metabolites with applications in the food industry using engineered microorganisms. Curr Opin Biotechnol 56:7–17

Kirst H, Formighieri C, Melis A (2014) Maximizing photosynthetic efficiency and culture productivity in cyanobacteria upon minimizing the phycobilisome light-harvesting antenna size. Biochim Biophys Acta 1837:1653–1664

Kiyota H, Okuda Y, Ito M, Hirai MY, Ikeuchi M (2014) Engineering of cyanobacteria for the photosynthetic production of limonene from CO_2. J Biotechnol 185:1–7

Kusakabe T, Tatsuke T, Tsuruno K, Hirokawa Y, Atsumi S, Liao JC, Hanai T (2013) Engineering a synthetic pathway in cyanobacteria for isopropanol production directly from carbon dioxide and light. Metab Eng 20:101–108

Lau NS, Matsui M, Abdullah AA (2015) Cyanobacteria: photoautotrophic microbial factories for the sustainable synthesis of industrial products. Biomed Res Int 2015:754934

Li H, Liao JC (2013) Engineering a cyanobacterium as the catalyst for the photosynthetic conversion of CO_2 to 1,2-propanediol. Microb Cell Fact 12. https://doi.org/10.1186/1475-2859-12-4

Lichtenthaler HK (1987) [34] Chlorophylls and carotenoids: pigments of photosynthetic biomembranes. Meth Enzymol 148:350–382

Lin PC, Pakrasi HB (2019) Engineering cyanobacteria for production of terpenoids. Planta 249:145–154

Lindberg P, Park S, Melis A (2010) Engineering a platform for photosynthetic isoprene production in cyanobacteria, using *Synechocystis* as the model organism. Metab Eng 12:70–79

Liu X, Sheng J, Curtiss R 3rd (2011) Fatty acid production in genetically modified cyanobacteria. Proc Natl Acad Sci U S A 108:6899–6904

Liu Y, Nielsen J (2019) Recent trends in metabolic engineering of microbial chemical factories. Curr Opin Biotechnol 60:188–197

Mavroudakis L, Valsami EA, Grafanaki S, Andreadaki TP, Ghanotakis DF, Pergantis SA (2019) The effect of nitrogen starvation on membrane lipids of *Synechocystis* sp. PCC 6803 investigated by using easy ambient sonic-spray ionization mass spectrometry. BBA-biomembranes 1861:183027

Melis A (2012) Photosynthesis-to-fuels: from sunlight to hydrogen, isoprene, and botryococcene production. Energy Environ Sci 5:5531–5539

Melis A (2017) Terpene hydrocarbons production in cyanobacteria. In: Los DA (ed) Cyanobacteria - Omics and manipulation. Caister Academic Press, NY pp 187–198

Miao R, Liu X, Englund E, Lindberg P, Lindblad P (2017) Isobutanol production in *Synechocystis* PCC 6803 using heterologous and endogenous alcohol dehydrogenases. Metab Eng Commun 5:45–53

Pattanaik B, Lindberg P (2015) Terpenoids and their biosynthesis in cyanobacteria. Life (Basel) 5:269–293

Reinsvold RE, Jinkerson RE, Radakovits R, Posewitz MC, Basu C (2011) The production of the sesquiterpene beta-caryophyllene in a transgenic strain of the cyanobacterium *Synechocystis*. J Plant Physiol 168:848–852

Santos-Merino M, Singh AK, Ducat DC (2019) New applications of synthetic biology tools for cyanobacterial metabolic engineering. Front Bioeng Biotechnol 7:33

Savakis P, Hellingwerf KJ (2015) Engineering cyanobacteria for direct biofuel production from CO_2. Curr Opin Biotechnol 33:8–14

Takahama K, Matsuoka M, Nagahama K, Ogawa T (2003) Construction and analysis of a recombinant cyanobacterium expressing a chromosomally inserted gene for an ethylene-forming enzyme at the psbAI locus. J Biosci Bioeng 95:302–305

Touloupakis E, Benavides AMS, Cicchi B, Torzillo G (2016) Growth and hydrogen production of outdoor cultures of *Synechocystis* PCC 6803. Algal Res 18:78–85

Van Wagoner RM, Drummond AK, Wright JL (2007) Biogenetic diversity of cyanobacterial metabolites. Adv Appl Microbiol 61:89–217

Xiong W, Morgan JA, Ungerer J, Wang B, Maness P-C, Yu J (2015) The plasticity of cyanobacterial metabolism supports direct CO_2 conversion to ethylene. Nat Plants 1:15053

Zhou J, Zhang H, Zhang Y, Li Y, Ma Y (2012) Designing and creating a modularized synthetic pathway in cyanobacterium *Synechocystis* enables production of acetone from carbon dioxide. Metab Eng 14:394–400

Zurbriggen A, Kirst H, Melis A (2012) Isoprene production via the mevalonic acid pathway in *Escherichia coli* (bacteria). BioEnergy Res 5: 814–828